

Search for New Physics in All-hadronic Events with AlphaT in 8 TeV data at CERN

Yossof Eshaq

*Submitted in Partial Fulfillment of the
Requirements for the Degree Doctor of Philosophy*

Supervised by Professor Aran Garcia-Bellido

Department of Physics

Astronomy

Arts, Sciences and Engineering

University of Rochester

September 19, 2014

Abstract

An inclusive search for supersymmetric processes that produce final states with jets and missing transverse energy is performed in pp collisions at a centre-of-mass energy of $\sqrt{s} = 8$ TeV. The data sample corresponds to an integrated luminosity of 18.5 fb^{-1} collected by the CMS experiment at the LHC. In this search, a dimensionless kinematic variable, α_T , is used to discriminate between events with genuine and misreconstructed missing transverse energy. The search is based on an examination of the number of reconstructed jets per event, the scalar sum of transverse energies of these jets, and the number of these jets identified as originating from bottom quarks. The results are interpreted with various simplified models, with a special emphasis on models with a compressed mass spectrum.

0.1 Theoretical motivation

SM,Higgs,SUSY

Particle physics concerns itself with the study of particles and fields. Our current knowledge of their characteristics and interactions are formalized in the quantum field theory called the Standard Model. It through three symmetries: The color charge symmetry of Quantum Chromo Dynamics (QCD) represented in $SU(3)$, the flavor symmetry of Quantum Flavor Dynamics (QFD) represented in $SU(2)$ and the electric charge symmetry of Quantum Electro Dynamics represented in $U(1)$. Together, $SU(3) \times SU(2) \times U(1)$ represent the field theory.

0.2 LHC and CMS

LHC, CMS

0.3 Definition of α_T AlphaT

0.4 Data sets and Monte Carlo samples

0.4.1 Data sets

0.4.2 MC samples for signal and SM backgrounds

0.4.3 Corrections to cross sections for SM samples

0.5 Triggers

0.5.1 Hadronic signal region

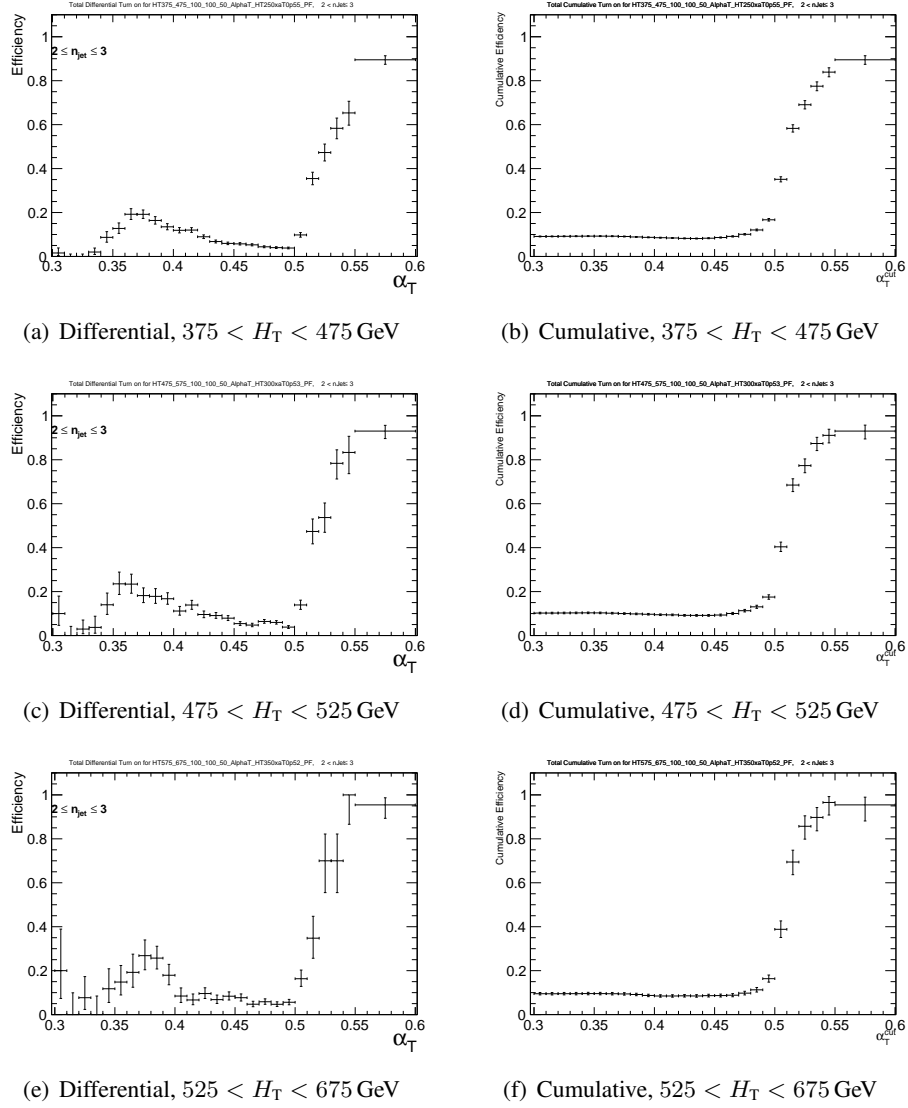


Figure 1: (Left) Differential and (Right) cumulative efficiency turn-on curves for the H_T - α_T cross triggers (as summarised in Table ??) that record events for the three lowest H_T bins for events satisfying $2 \leq n_{\text{jet}} \leq 3$.

0.5.2 Muon control samples

0.6 Physics objects

The definitions of the physics objects used in this analysis follow the recommendations of the various Physics Object Groups (POGs).

0.6.1 Jets

0.6.2 b-tagged jets

0.6.3 Muons

0.6.4 Photons

0.6.5 Electrons

0.6.6 Single isolated tracks

0.7 Event selection

0.7.1 Event vetoes for leptons, photons, and single isolated tracks

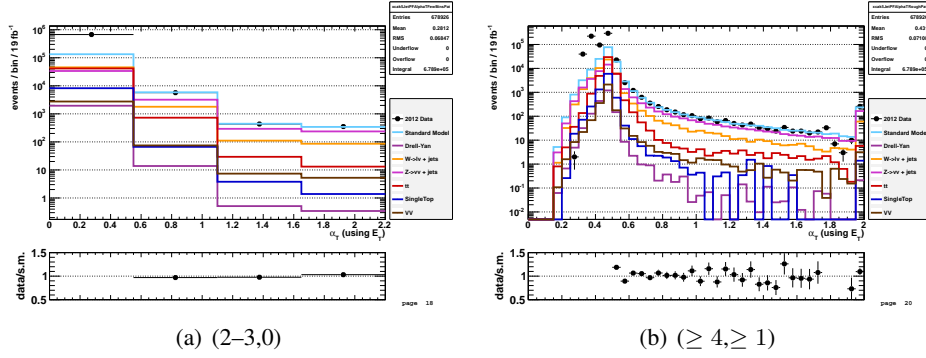


Figure 2: Data–MC comparison of the α_T distribution for the hadronic signal region, following the application of the hadronic pre-selection criteria and the requirements $H_T > 375$ GeV and $\alpha_T > 0.55$, for events satisfying (Left) $2 \leq n_{\text{jet}} \leq 3$ and $n_b = 0$ and (Right) $n_{\text{jet}} \geq 4$ and $n_b \geq 1$. Bands represent the uncertainties due to the limited size of MC samples.

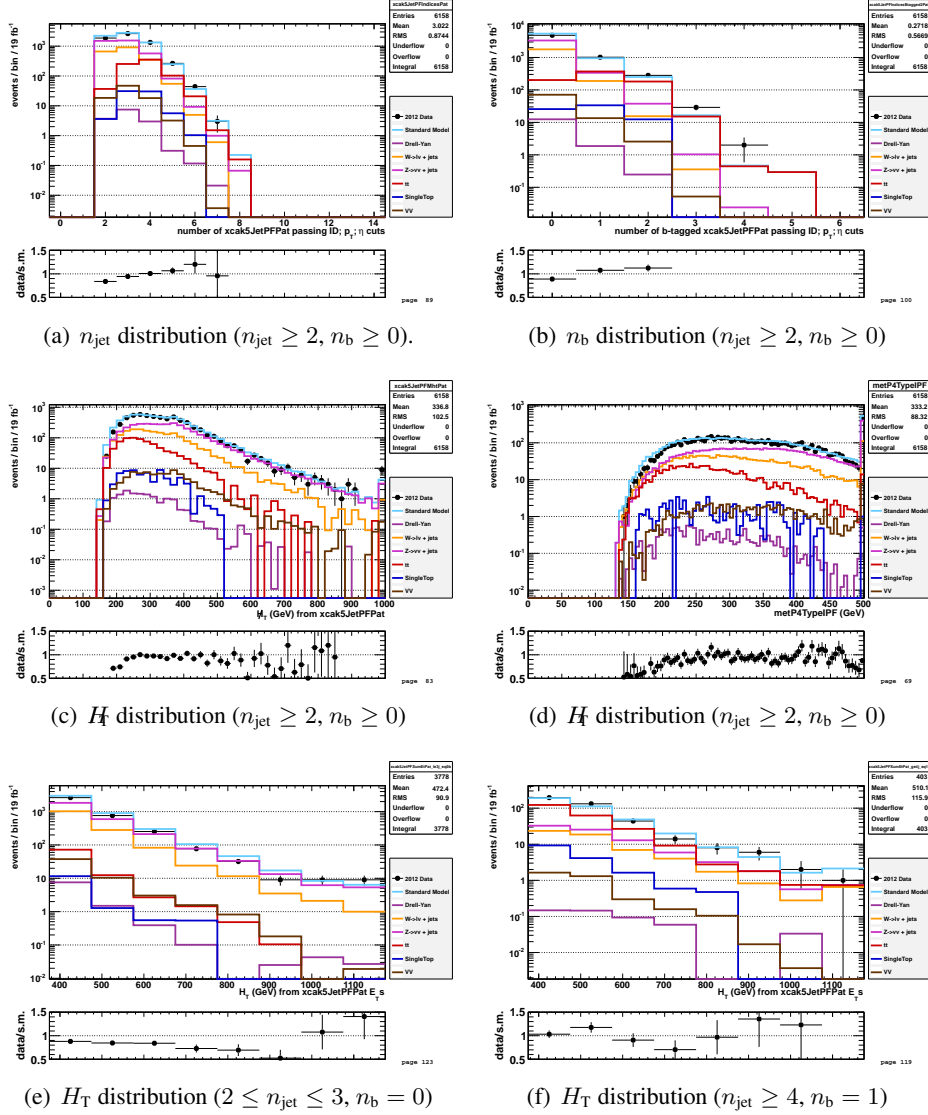


Figure 3: Data–MC comparisons of key variables for the hadronic signal region, following the application of the full signal region selection criteria and the requirements $H_T > 375$ GeV and $\alpha_T > 0.55$: (a) n_{jet} , (b) n_b , (c) H_T , and (d) E_T distributions for an inclusive selection on n_{jet} and n_b , and (e,f) H_T for the two event categories ($2 \leq n_{\text{jet}} \leq 3, n_b = 0$) and ($n_{\text{jet}} \geq 4, n_b = 1$).

0.8 Closure tests and systematic uncertainties on transfer factors

Since the transfer factors are obtained from simulation, an appropriate systematic uncertainty is assigned to each factor to account for theoretical uncertainties [?] and limitations in the simulation modelling of event kinematics and instrumental effects. This section describes how the systematic uncertainties are determined from closure tests in data.

0.8.1 Closure tests

Table 1: $2 \leq n_{\text{jet}} \leq 3$ bin.

Closure test	Symbol	Constant fit			
		Best fit value	χ^2	d.o.f.	p -value
$\alpha_T < 0.55 \rightarrow \alpha_T > 0.55$ (μ + jets)	Circle	0.007 ± 0.02	3.91	7	0.79
$2 \leq n_{\text{jet}} \leq 3 \rightarrow n_{\text{jet}} \geq 4$ (μ + jets, 1 b-tags)	Times	-0.053 ± 0.03	8.02	7	0.33
$2 \leq n_{\text{jet}} \leq 3 \rightarrow n_{\text{jet}} \geq 4$ (μ + jets, 1 b-tags)	Invert. Triangle	0.018 ± 0.04	6.23	7	0.51
$2 \leq n_{\text{jet}} \leq 3 \rightarrow n_{\text{jet}} \geq 4$ (μ + jets, 0 b-tags)	Star	0.034 ± 0.02	9.24	7	0.24
$2 \leq n_{\text{jet}} \leq 3 \rightarrow n_{\text{jet}} \geq 4$ (γ + jets, 0 b-tags)	Diamond	0.100 ± 0.04	12.20	7	0.09
1 b-tags \rightarrow 2 b-tags (μ + jets, nJet=3)	Triangle	-0.008 ± 0.04	3.20	7	0.87
0 b-tags \rightarrow 1 b-tags (μ + jets, nJet=2)	Cross	0.111 ± 0.03	5.87	7	0.55
0 b-tags \rightarrow 1 b-tags (μ + jets, nJet=3)	Square	0.040 ± 0.02	1.12	7	0.99

Table 2: $n_{\text{jet}} \geq 4$ bin.

Closure test	Symbol	Constant fit			
		Best fit value	χ^2	d.o.f.	p -value
$\alpha_T < 0.55 \rightarrow \alpha_T > 0.55$ (μ + jets)	Circle	0.011 ± 0.04	5.81	7	0.56
$2 \leq n_{\text{jet}} \leq 3 \rightarrow n_{\text{jet}} \geq 4$ (μ + jets, 1 b-tags)	Times	-0.053 ± 0.03	8.02	7	0.33
$2 \leq n_{\text{jet}} \leq 3 \rightarrow n_{\text{jet}} \geq 4$ (μ + jets, 1 b-tags)	Invert. Triangle	0.018 ± 0.04	6.23	7	0.51
$2 \leq n_{\text{jet}} \leq 3 \rightarrow n_{\text{jet}} \geq 4$ (μ + jets, 0 b-tags)	Star	0.034 ± 0.02	9.24	7	0.24
$2 \leq n_{\text{jet}} \leq 3 \rightarrow n_{\text{jet}} \geq 4$ (γ + jets, 0 b-tags)	Diamond	0.100 ± 0.04	12.20	7	0.09
1 b-tags \rightarrow 2 b-tags (μ + jets)	Triangle	0.045 ± 0.03	9.36	7	0.23
0 b-tags \rightarrow 1 b-tags (μ + jets)	Square	0.007 ± 0.03	25.30	7	0.00

Table 3: A summary of the magnitude of the systematic uncertainties (%) assigned to the transfer factors, according to n_{jet} and H_{T} region.

n_{jet}	H_{T} region (GeV)							
	375–475	475–525	525–675	675–775	775–875	875–975	1075–1075	> 1175
2–3	3	4	5	11	11	16	16	16
≥ 4	3	4	6	13	13	13	13	20

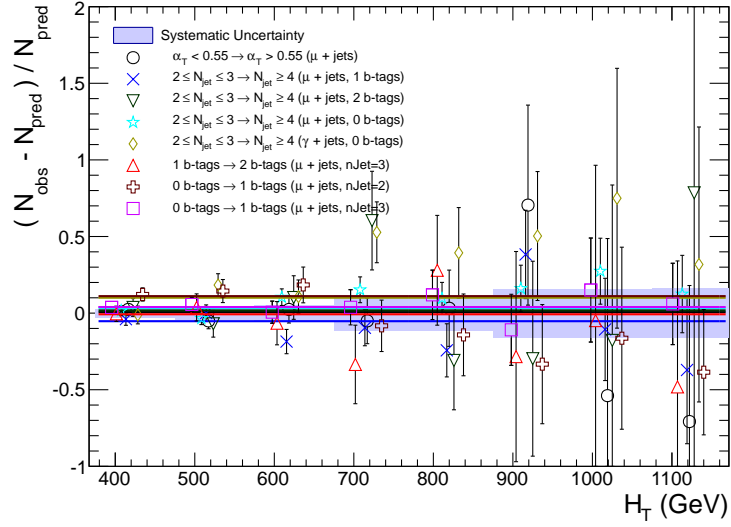
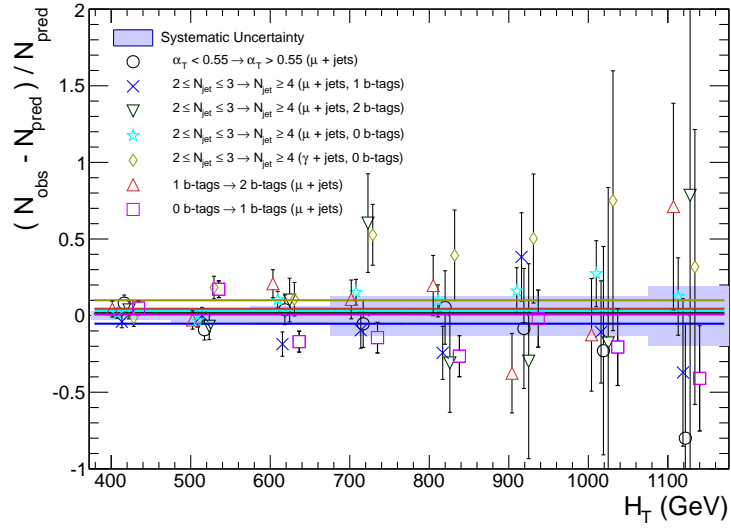
(a) $2 \leq n_{\text{jet}} \leq 3$ (b) $n_{\text{jet}} \geq 4$

Figure 4: Sets of closure tests (open symbols) overlaid on top of the systematic uncertainty used for each of the five H_T regions (shaded bands) and for the two different jet multiplicity bins: (a) $2 \leq n_{\text{jet}} \leq 3$ and (b) $n_{\text{jet}} \geq 4$.

0.9 Results

0.9.1 Standard Model

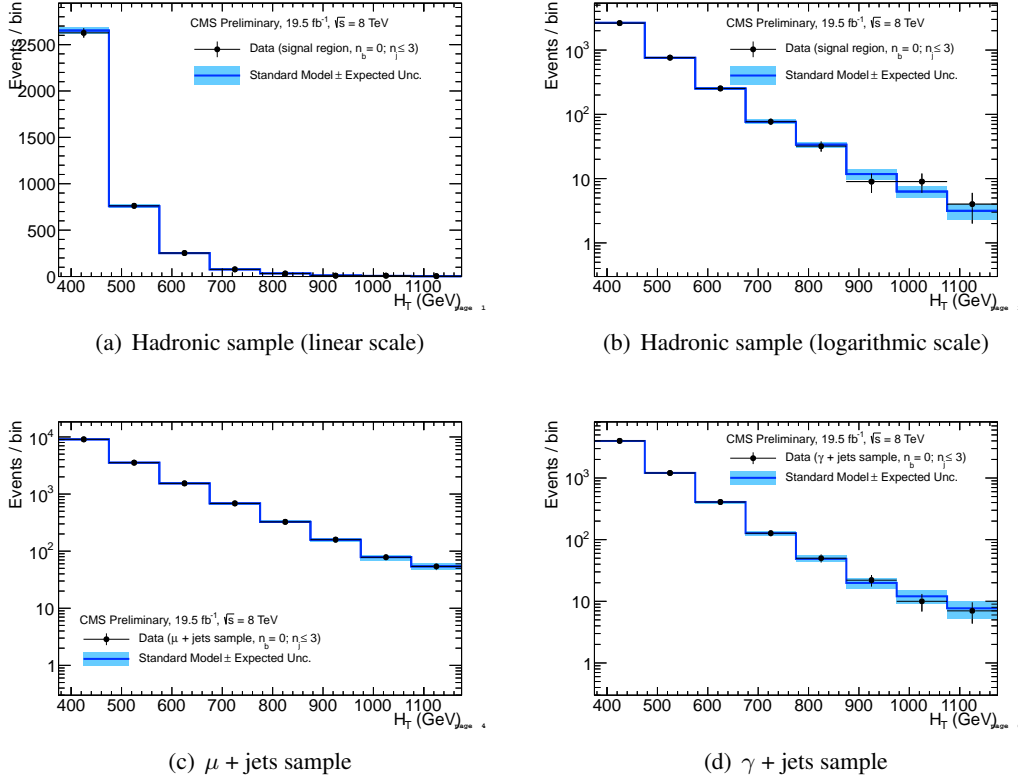


Figure 5: Comparison of the H_T -binned observed data yields and SM expectations when requiring $2 \leq n_{\text{jet}} \leq 3$ and $n_b = 0$ for the (a-b) hadronic, (c) μ + jets, (d) $\mu\mu$ + jets and (e) γ + jets samples, as determined by a simultaneous fit to all data samples under the SM-only hypothesis. The observed event yields in data (black dots) and the expectations and their uncertainties (dark blue solid line with light blue bands), as determined by the simultaneous fit, are shown. For illustrative purposes only, the signal expectations (pink dashed line) for the model T2cc with $m_{\tilde{q}} = 250$ GeV and $m_{\text{LSP}} = 240$ GeV are stacked on top of the SM expectations.

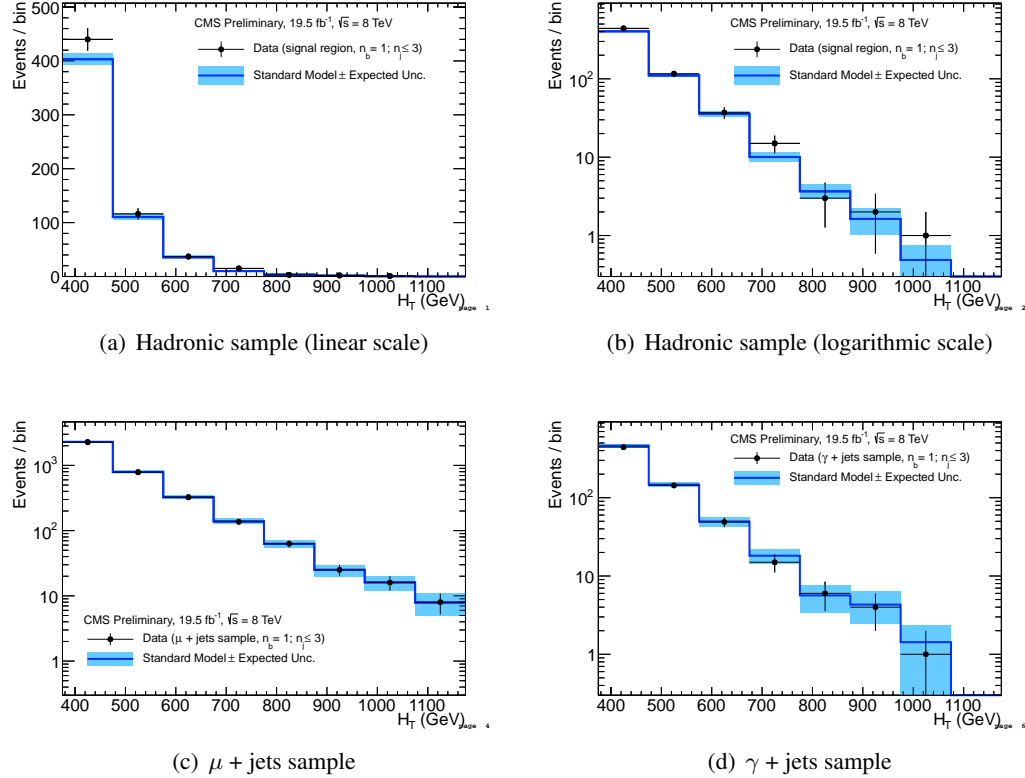


Figure 6: Comparison of the H_T -binned observed data yields and SM expectations when requiring $2 \leq n_{\text{jet}} \leq 3$ and $n_b = 1$ for the (a-b) hadronic, (c) $\mu + \text{jets}$, (d) $\mu\mu + \text{jets}$ and (e) $\gamma + \text{jets}$ samples, as determined by a simultaneous fit to all data samples under the SM-only hypothesis. The observed event yields in data (black dots) and the expectations and their uncertainties (dark blue solid line with light blue bands), as determined by the simultaneous fit, are shown. For illustrative purposes only, the signal expectations (pink dashed line) for the model T2cc with $m_{\tilde{q}} = 250$ GeV and $m_{\text{LSP}} = 170$ GeV are stacked on top of the SM expectations.

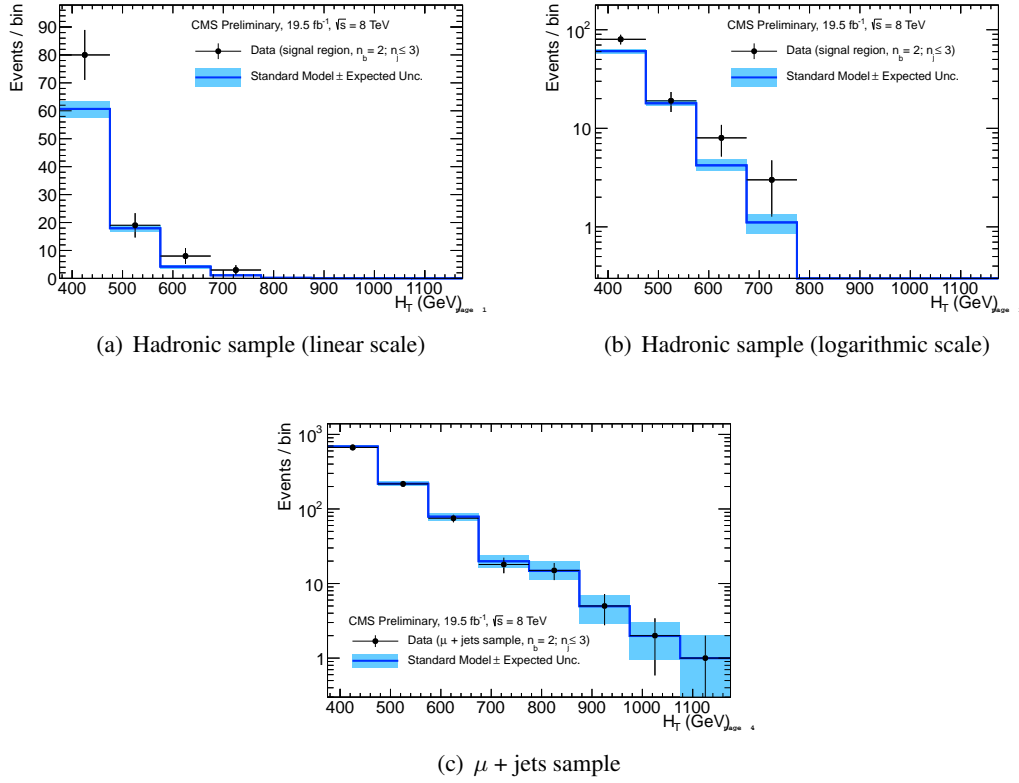


Figure 7: Comparison of the H_T -binned observed data yields and SM expectations when requiring $2 \leq n_{jet} \leq 3$ and $n_b = 2$ for the (a-b) hadronic and μ + jets samples, as determined by a simultaneous fit to both the hadronic and μ + jets data samples under the SM-only hypothesis. The observed event yields in data (black dots) and the expectations and their uncertainties (dark blue solid line with light blue bands), as determined by the simultaneous fit, are shown.

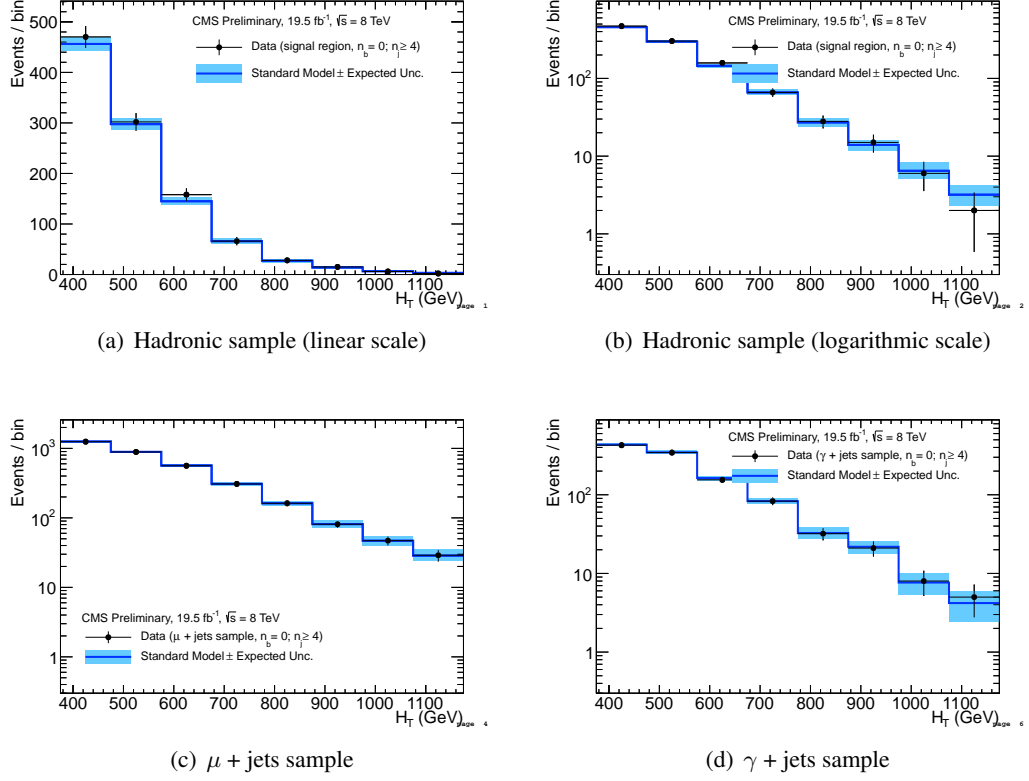


Figure 8: Comparison of the H_T -binned observed data yields and SM expectations when requiring $n_{\text{jet}} \geq 4$ and $n_b = 0$ for the (a-b) hadronic, (c) μ + jets, (d) $\mu\mu$ + jets and (e) γ + jets samples, as determined by a simultaneous fit to all data samples under the SM-only hypothesis. The observed event yields in data (black dots) and the expectations and their uncertainties (dark blue solid line with light blue bands), as determined by the simultaneous fit, are shown. For illustrative purposes only, the signal expectations (pink dashed line) for the model T2cc with $m_{\tilde{q}} = 250$ GeV and $m_{\text{LSP}} = 170$ GeV are stacked on top of the SM expectations.

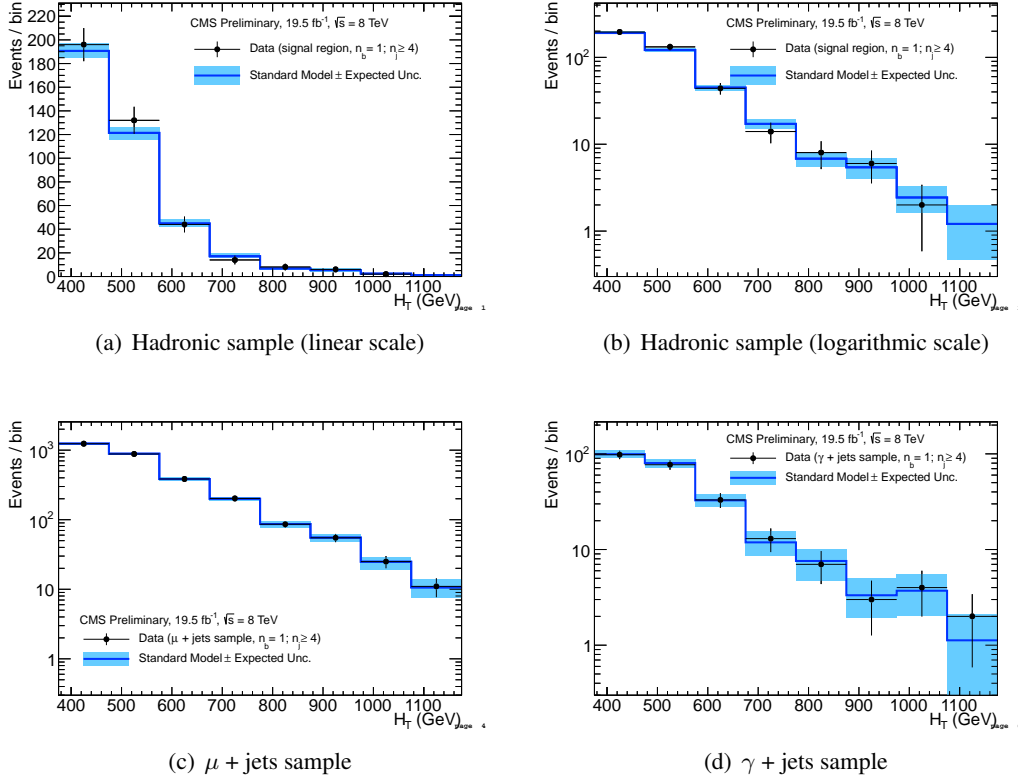


Figure 9: Comparison of the H_T -binned observed data yields and SM expectations when requiring $n_{\text{jets}} \geq 4$ and $n_b = 1$ for the (a-b) hadronic, (c) $\mu + \text{jets}$, (d) $\mu\mu + \text{jets}$ and (e) $\gamma + \text{jets}$ samples, as determined by a simultaneous fit to all data samples under the SM-only hypothesis. The observed event yields in data (black dots) and the expectations and their uncertainties (dark blue solid line with light blue bands), as determined by the simultaneous fit, are shown. For illustrative purposes only, the signal expectations (pink dashed line) for the model T2cc with $m_{\tilde{q}} = 250$ GeV and $m_{\text{LSP}} = 170$ GeV are stacked on top of the SM expectations.

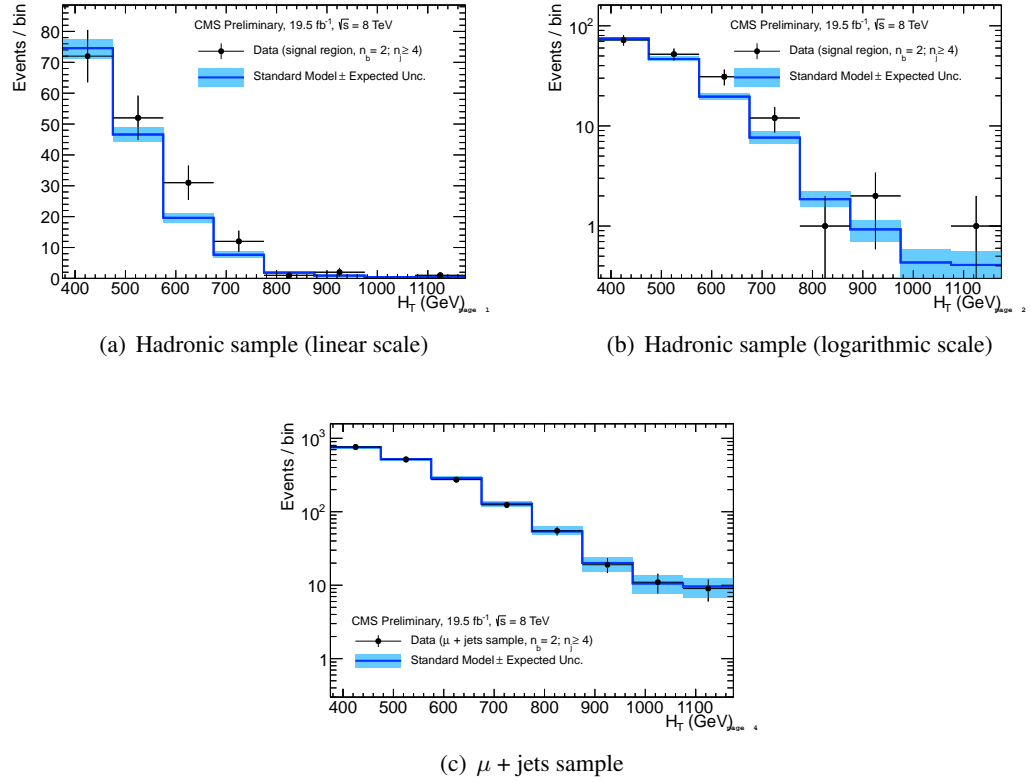
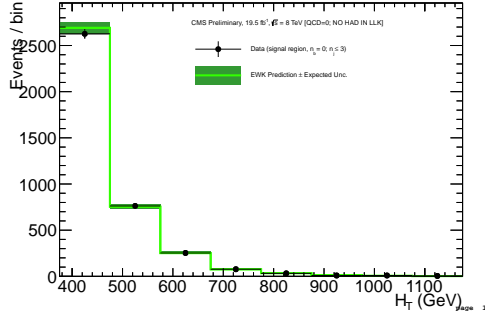
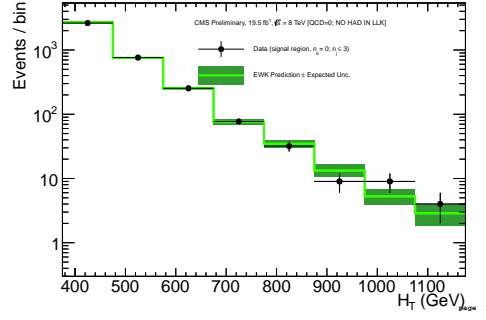


Figure 10: Comparison of the H_T -binned observed data yields and SM expectations when requiring $n_{jet} \geq 4$ and $n_b = 2$ for the (a-b) hadronic and μ + jets samples, as determined by a simultaneous fit to both the hadronic and μ + jets data samples under the SM-only hypothesis. The observed event yields in data (black dots) and the expectations and their uncertainties (dark blue solid line with light blue bands), as determined by the simultaneous fit, are shown.



(a) Hadronic sample (linear scale)



(b) Hadronic sample (logarithmic scale)

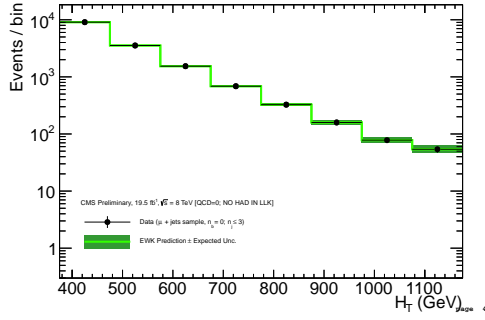
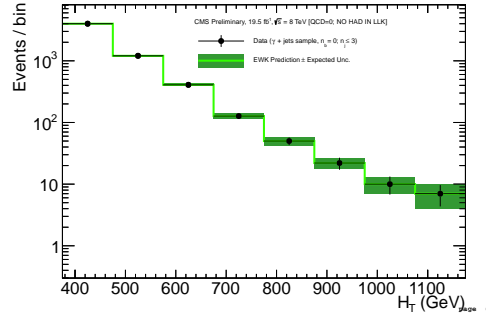
(c) μ + jets sample(d) γ + jets sample

Figure 11: Comparison of the H_T -binned observed data yields and SM expectations when requiring $2 \leq n_{\text{jet}} \leq 3$ and $n_b = 0$ for the (a-b) hadronic, (c) μ + jets, (d) $\mu\mu$ + jets and (e) γ + jets samples, as determined by a simultaneous fit to the data control samples only. The observed event yields in data (black dots) and the expectations and their uncertainties (dark green solid line with light green bands), as determined by the simultaneous fit, are shown.

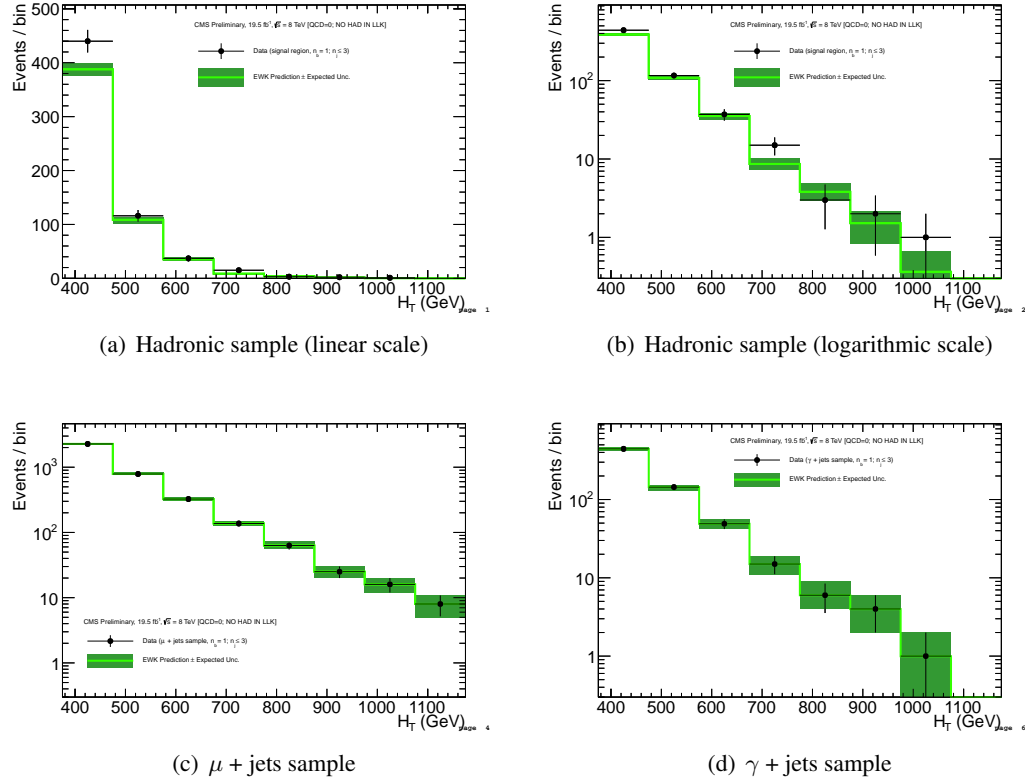


Figure 12: Comparison of the H_T -binned observed data yields and SM expectations when requiring $2 \leq n_{\text{jet}} \leq 3$ and $n_b = 1$ for the (a-b) hadronic, (c) μ + jets, (d) $\mu\mu$ + jets and (e) γ + jets samples, as determined by a simultaneous fit to the data control samples only. The observed event yields in data (black dots) and the expectations and their uncertainties (dark green solid line with light green bands), as determined by the simultaneous fit, are shown.

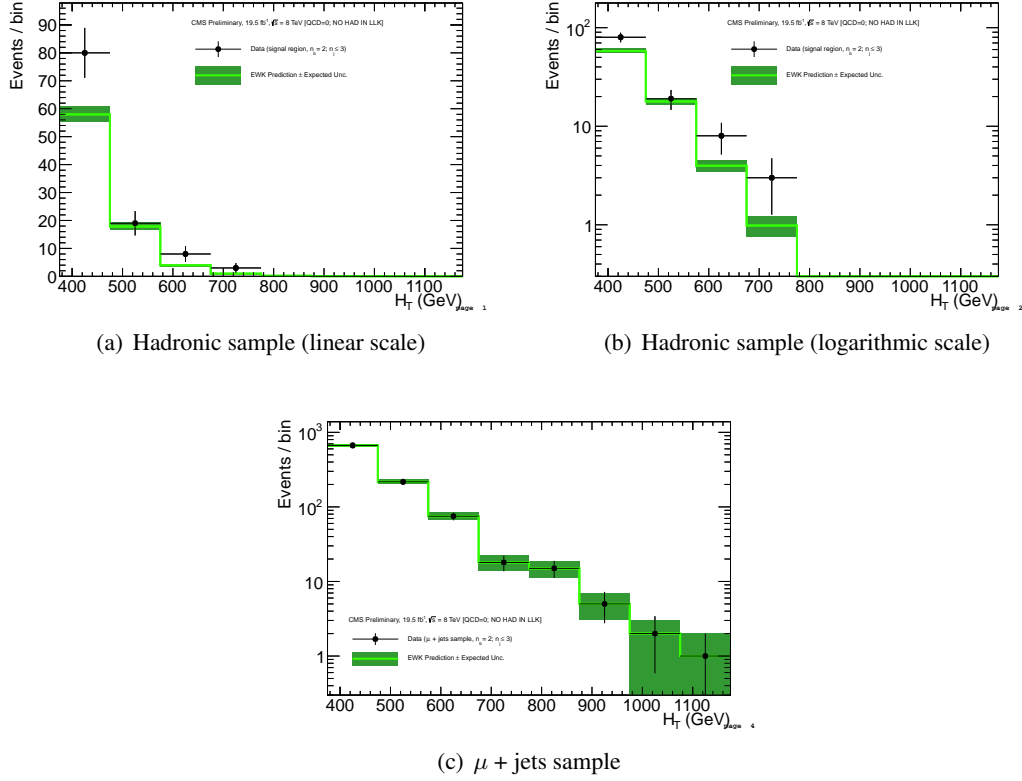


Figure 13: Comparison of the H_T -binned observed data yields and SM expectations when requiring $2 \leq n_{\text{jet}} \leq 3$ and $n_b = 2$ for the (a-b) hadronic, (c) $\mu + \text{jets}$, (d) $\mu\mu + \text{jets}$ and (e) $\gamma + \text{jets}$ samples, as determined by the $\mu + \text{jets}$ data control sample only. The observed event yields in data (black dots) and the expectations and their uncertainties (dark green solid line with light green bands) are shown.

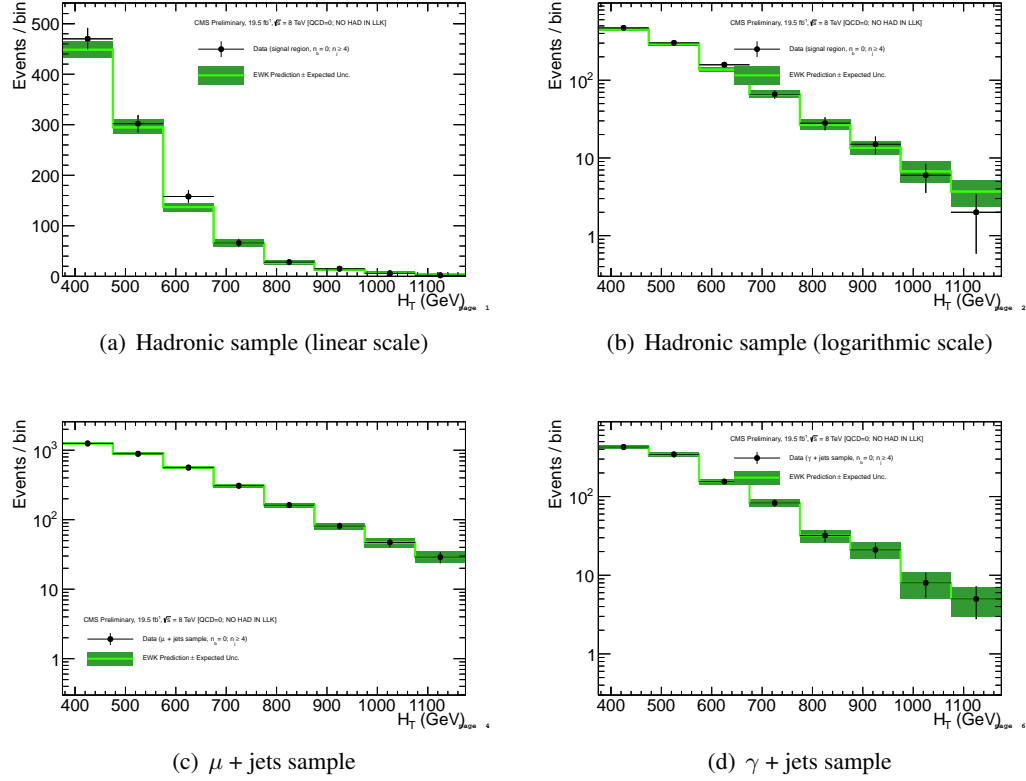
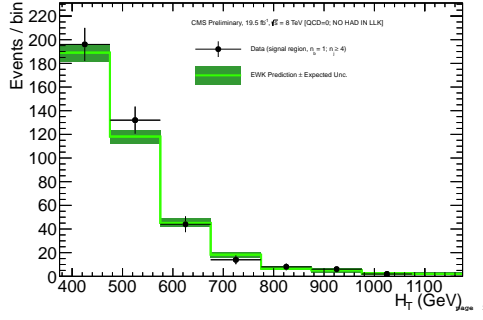
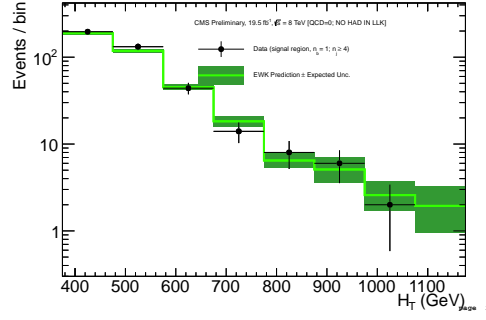


Figure 14: Comparison of the H_T -binned observed data yields and SM expectations when requiring $n_{\text{jet}} \geq 4$ and $n_b = 0$ for the (a-b) hadronic, (c) μ + jets, (d) $\mu\mu$ + jets and (e) γ + jets samples, as determined by a simultaneous fit to the data control samples only. The observed event yields in data (black dots) and the expectations and their uncertainties (dark green solid line with light green bands), as determined by the simultaneous fit, are shown.



(a) Hadronic sample (linear scale)



(b) Hadronic sample (logarithmic scale)

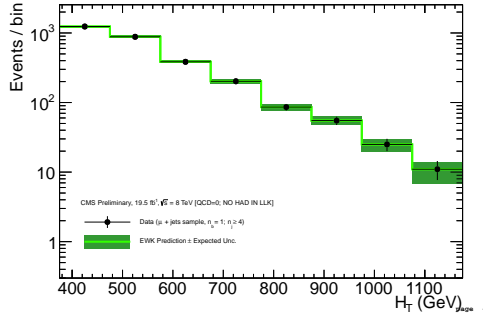
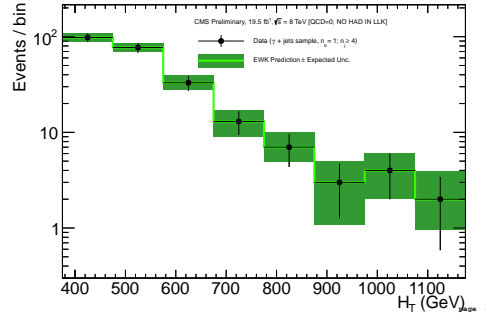
(c) μ + jets sample(d) γ + jets sample

Figure 15: Comparison of the H_T -binned observed data yields and SM expectations when requiring $n_{jet} \geq 4$ and $n_b = 1$ for the (a-b) hadronic, (c) μ + jets, (d) $\mu\mu$ + jets and (e) γ + jets samples, as determined by a simultaneous fit to the data control samples only. The observed event yields in data (black dots) and the expectations and their uncertainties (dark green solid line with light green bands), as determined by the simultaneous fit, are shown.

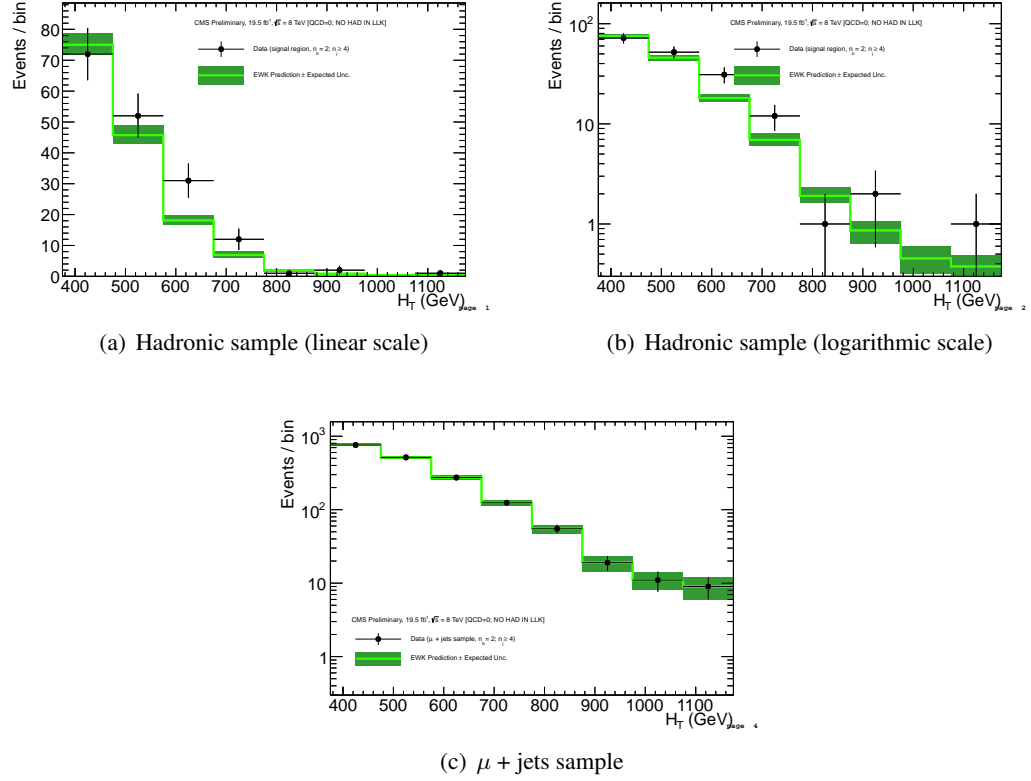


Figure 16: Comparison of the H_T -binned observed data yields and SM expectations when requiring $n_{\text{jet}} \geq 4$ and $n_b = 2$ for the (a-b) hadronic, (c) μ + jets, (d) $\mu\mu$ + jets and (e) γ + jets samples, as determined by the μ + jets data control sample only. The observed event yields in data (black dots) and the expectations and their uncertainties (dark green solid line with light green bands) are shown.

.1 SM-only yield tables

The following tables compare the observations in the hadronic and control samples with the maximum-likelihood expectations obtained by the SM-only fit.

Table 4: 0b le3j

H_T Bin (GeV)	375–475	475–575	575–675	675–775	775–875	875–975	975–1075	1075– ∞
SM hadronic	2652^{+33}_{-41}	758^{+20}_{-18}	252^{+10}_{-12}	$76.5^{+6.1}_{-5.0}$	$33.7^{+3.2}_{-3.3}$	$11.8^{+2.0}_{-2.2}$	$6.3^{+1.4}_{-1.3}$	$3.2^{+0.9}_{-0.9}$
Data hadronic	2627	762	253	77	32	9	9	4
SM μ +jets	9069^{+77}_{-115}	3546^{+51}_{-59}	1538^{+33}_{-39}	686^{+22}_{-27}	325^{+18}_{-16}	158^{+12}_{-13}	$78.6^{+6.2}_{-9.4}$	$54.1^{+7.5}_{-7.3}$
Data μ +jets	9078	3545	1538	686	326	159	78	54
SM γ +jets	3984^{+56}_{-59}	1209^{+34}_{-35}	408^{+17}_{-22}	127^{+10}_{-9}	$48.8^{+6.0}_{-5.5}$	$19.9^{+3.8}_{-3.9}$	$12.1^{+2.8}_{-3.1}$	$7.7^{+2.4}_{-2.5}$
Data γ +jets	4000	1206	408	127	50	22	10	7

Table 5: 0b ge4j

H_T Bin (GeV)	375–475	475–575	575–675	675–775	775–875	875–975	975–1075	1075– ∞
SM hadronic	456^{+13}_{-14}	298^{+12}_{-12}	145^{+7}_{-7}	$66.0^{+5.5}_{-4.7}$	$27.1^{+3.8}_{-3.1}$	$13.9^{+2.2}_{-2.1}$	$6.5^{+1.8}_{-1.4}$	$3.2^{+1.0}_{-0.9}$
Data hadronic	470	302	158	66	28	15	6	2
SM μ +jets	1256^{+30}_{-41}	890^{+28}_{-30}	567^{+22}_{-23}	308^{+18}_{-15}	162^{+12}_{-12}	$81.3^{+9.9}_{-9.3}$	$46.9^{+7.8}_{-6.5}$	$28.6^{+6.7}_{-4.8}$
Data μ +jets	1249	888	562	308	162	81	47	29
SM γ +jets	434^{+19}_{-18}	347^{+15}_{-18}	163^{+12}_{-11}	$83.0^{+6.8}_{-7.5}$	$32.6^{+6.3}_{-5.0}$	$21.8^{+4.1}_{-4.1}$	$7.7^{+2.5}_{-2.3}$	$4.2^{+1.8}_{-1.8}$
Data γ +jets	427	344	155	83	32	21	8	5

Table 6: 1b le3j

H_T Bin (GeV)	375–475	475–575	575–675	675–775	775–875	875–975	975–1075	1075– ∞
SM hadronic	403^{+12}_{-10}	110^{+6}_{-5}	$35.8^{+2.9}_{-2.9}$	$10.0^{+1.5}_{-1.3}$	$3.7^{+0.8}_{-0.8}$	$1.6^{+0.6}_{-0.6}$	$0.5^{+0.3}_{-0.3}$	$0.1^{+0.1}_{-0.0}$
Data hadronic	440	116	37	15	3	2	1	0
SM μ +jets	2291^{+50}_{-48}	790^{+31}_{-25}	326^{+20}_{-16}	139^{+13}_{-11}	$62.7^{+8.3}_{-7.4}$	$25.1^{+4.7}_{-5.0}$	$16.1^{+3.9}_{-4.2}$	$7.9^{+3.0}_{-3.0}$
Data μ +jets	2272	787	325	137	63	25	16	8
SM γ +jets	461^{+22}_{-22}	147^{+10}_{-10}	$49.7^{+6.5}_{-6.7}$	$18.1^{+4.0}_{-3.6}$	$5.6^{+2.0}_{-2.2}$	$4.3^{+2.0}_{-1.9}$	$1.4^{+0.9}_{-1.4}$	$0.0^{+0.0}_{-0.0}$
Data γ +jets	444	144	49	15	6	4	1	0

Table 7: 1b ge4j

H_T Bin (GeV)	375–475	475–575	575–675	675–775	775–875	875–975	975–1075	1075– ∞
SM hadronic	191^{+6}_{-6}	121^{+5}_{-5}	$44.8^{+3.3}_{-2.8}$	$17.1^{+2.3}_{-1.9}$	$6.8^{+1.1}_{-1.3}$	$5.4^{+1.5}_{-1.4}$	$2.4^{+0.8}_{-0.8}$	$1.2^{+0.8}_{-0.7}$
Data hadronic	196	132	44	14	8	6	2	0
SM μ +jets	1242^{+37}_{-34}	888^{+27}_{-26}	384^{+21}_{-18}	200^{+14}_{-12}	$86.6^{+9.1}_{-10.0}$	$55.2^{+7.4}_{-6.2}$	$24.9^{+4.6}_{-5.7}$	$10.6^{+3.3}_{-3.0}$
Data μ +jets	1238	881	385	202	86	55	25	11
SM γ +jets	$99.2^{+9.5}_{-8.6}$	$80.2^{+7.9}_{-8.7}$	$32.7^{+5.7}_{-4.6}$	$11.9^{+3.4}_{-3.3}$	$7.6^{+2.3}_{-2.9}$	$3.3^{+1.7}_{-1.4}$	$3.7^{+1.8}_{-1.7}$	$1.1^{+1.0}_{-1.0}$
Data γ +jets	98	77	33	13	7	3	4	2

Table 8: 2b le3j

H_T Bin (GeV)	375–475	475–575	575–675	675–775	775–875	875–975	975–1075	1075– ∞
SM hadronic	$60.7^{+2.9}_{-3.1}$	$18.0^{+1.3}_{-1.2}$	$4.2^{+0.6}_{-0.5}$	$1.1^{+0.2}_{-0.2}$	$0.2^{+0.1}_{-0.1}$	$0.0^{+0.0}_{-0.0}$	$0.0^{+0.0}_{-0.0}$	$0.0^{+0.0}_{-0.0}$
Data hadronic	80	19	8	3	0	0	0	0
SM μ +jets	687^{+23}_{-26}	218^{+14}_{-14}	$78.8^{+9.1}_{-8.5}$	$19.9^{+3.9}_{-3.9}$	$14.8^{+4.9}_{-3.8}$	$5.0^{+2.0}_{-2.1}$	$2.0^{+1.0}_{-1.0}$	$1.0^{+1.0}_{-1.0}$
Data μ +jets	668	217	75	18	15	5	2	1

Table 9: 2b ge4j

H_T Bin (GeV)	375–475	475–575	575–675	675–775	775–875	875–975	975–1075	1075– ∞
SM hadronic	$74.6^{+3.0}_{-3.5}$	$46.6^{+2.5}_{-2.3}$	$19.6^{+1.6}_{-1.4}$	$7.6^{+1.2}_{-1.1}$	$1.9^{+0.4}_{-0.3}$	$0.9^{+0.2}_{-0.2}$	$0.4^{+0.1}_{-0.1}$	$0.4^{+0.2}_{-0.1}$
Data hadronic	72	52	31	12	1	2	0	1
SM μ +jets	757^{+23}_{-28}	520^{+23}_{-21}	285^{+18}_{-15}	128^{+10}_{-10}	$54.1^{+8.8}_{-5.8}$	$20.1^{+4.1}_{-4.7}$	$10.6^{+3.0}_{-3.0}$	$9.6^{+2.9}_{-2.9}$
Data μ +jets	760	515	274	124	55	19	11	9

Bibliography

- [1] S. Chatrchyan et al. Missing transverse energy performance of the cms detector. *JINST*, 6:P09001, 2011.
- [2] Serguei Chatrchyan et al. Determination of Jet Energy Calibration and Transverse Momentum Resolution in CMS. *JINST*, 6:P11002, 2011.
- [3] V. Khachatryan et al. Search for Supersymmetry in pp Collisions at 7 TeV in Events with Jets and Missing Transverse Energy. *Phys. Lett. B*, 698:196, 2011.
- [4] L. Randall and D. Tucker-Smith. Dijet searches for supersymmetry at the large hadron collider. *Phys. Rev. Lett.*, 101:221803, 2008.